Snow cornice and snow avalanche monitoring using automatic time lapse cameras in Tasiapik Valley, Nunavik (Québec) during the winter of 2017–2018

Samuel Veilleux, Armelle Decaulne, Najat Bhiry

Snow cornice and snow avalanche monitoring using automatic time lapse cameras in Tasiapik Valley, Nunavik (Québec) during the winter of 2017–2018

Samuel Veilleux, Armelle Decaulne, and Najat Bhiry

Abstract: A series of automatic time-lapse cameras installed along the southwestern side of Tasiapik Valley, near the village of Umiujaq, Nunavik (northern Québec) documented several departure modes and types of snow involved in snow avalanches during winter 2017–2018. These included cornice–avalanche dynamics, slab and loose snow avalanches, and clean and dirty snow avalanches. At the top of the selected slope, a camera monitored the development of a snow cornice beginning in November 2017, detecting multiple cornice failures over the winter and spring. The track and deposition area of the runout paths were monitored from two cameras downslope, revealing the concomitance of snow–cornice fall and snow avalanche triggering. Snow avalanche activity remained relatively infrequent until the end of May 2018. Spring snow avalanche activity is characterized by wet and dirty snow avalanches carrying debris to the foot of the slope and by runout zones located near the road along the slope.

Key words: snow avalanche, snow cornice, failure, slopes, Nunavik.

Résumé : Des caméras à déclenchement automatique installées le long du versant sud-ouest de la vallée Tasiapik, près du village d'Umiujaq, au Nunavik (Nord du Québec) ont permis de documenter de nombreux événements d'avalanche, leurs différents modes de départ et les types de dépôts impliqués au cours de l'hiver 2017–2018. Une dynamique corniche-avalanche a pu être observée, en plus des avalanches de plaque et de neige sans cohésion, et des dépôts de neige propre et sale. Au sommet du versant, une caméra a suivi le développement d'une corniche de neige à partir de novembre 2017, ainsi que les nombreuses ruptures de corniche au cours de l'hiver et au printemps. Deux autres caméras ont suivi l'évolution de la dynamique avalancheuse depuis la base du versant. Une synchronicité entre les effondrements de corniche et le déclenchement des avalanches a été observée. L'activité avalancheuse est demeurée faible jusqu'à la fin mai 2018. Les avalanches printanières à la fin mai et en juin se caractérisent par une neige mouillée et sale transportant des débris au pied des pentes, ne s'arrêtant parfois qu'à quelques mètres de la route longeant le versant.

Mots-clés : avalanche, corniche de neige, chute, versant, Nunavik.

Received 5 May 2020. Accepted 13 January 2021.

S. Veilleux and N. Bhiry. Département de géographie and Centre d'études nordiques, Université Laval, Québec, QC G1V 0A6, Canada.
A. Decaulne. CNRS, Laboratoire LETG, Université de Nantes, LabEx DRIIHM, 44312 Nantes, France.
Corresponding author: Samuel Veilleux (e-mail: samuel.veilleux.4@ulaval.ca).

Introduction

Snow avalanches are a known hazard for some Inuit communities in Nunavik, as noted by Lied and Domaas (2000) in their report for Québec's Ministry of Public Security after the deadly avalanche that occurred on 1 January 1999 in Kangiqsualujjuaq. Their investigation focused on the villages of Inukjuak, Ivujivik, Kangiqsualujjuaq, Kangiqsujuaq, Kangirsuk, Quaqtaq, and Salluit, located in glacial valleys where steep slopes are bordering the buildings. However, for other villages such as Umiujaq, where the slopes are located at a distance from the built-up areas, this natural hazard is not sufficiently documented, as it has never been studied in the area before. Moreover, the risk for local populations remains poorly acknowledged, as no study has described the occurrence or triggering mechanisms of snow avalanches in this area (Hétu 2001; Germain 2016). According to Germain (2016), environmental conditions in Nunavik are favourable for snow avalanches; these conditions include strong winds, snowfall, and steep, bare slopes heavily weathered by strong periglacial activity. Thus, in the context of changing climatic and meteorological conditions, it is necessary to document snow avalanches and their impacts.

Using time lapse photography, in situ observation, and meteorological data, this paper aims to examine the occurrence and triggering events of snow avalanches in Tasiapik Valley (near Umiujaq), in relation to the impact of the prevailing meteorological conditions and topographic parameters on the evolution of snow cover instability. As the data and observations presented in this paper cover the first year of snow avalanche monitoring in Tasiapik Valley, they should be considered as a preliminary investigation of this specific case study.

Study site

Tasiapik Valley (56°33′N, 76°28′W) is located 5 km east of the Inuit village of Umiujaq, on the eastern shore of Hudson Bay in Nunavik, Québec (Fig. 1A).

The valley is approximately 4.5 km long and 1.5 km wide, following a northwest–southeast orientation. Downstream of the valley lies Tasiujaq Lake (formerly named Guillaume-Delisle Lake and Richmond Gulf), a brackish 691 km^2 lake connected with Hudson Bay (ARK 2007). This area is frequently visited by the local population for traditional activities, but also by scientists and more recently by tourists (Tursujuq National Park).

The area is characterized by a cuesta relief, revealing a gentle conform west-dipping slope and a steep eastern frontslope (Dionne 1976; Guimont and Laverdière 1980). The "Hudson Bay cuestas" consist of a Paleoproterozoic volcanic–sedimentary sequence lying unconformably on the Precambrian shield (Stockwell et al. 1979; Chandler and Schwarz 1980; Chandler 1988; Eaton and Darbyshire 2010). Tasiapik Valley is bordered on the southwest by the cuesta; the height of the cuesta slope increases southward along the valley towards Tasiujaq Lake from 50 to 230 m (Fig. 1B). Veilleux et al. (2020) documented the occurrence of rockfalls and snow avalanches at this precise location from morphometric studies on the talus and cones in the distal part of the slope, snow avalanches being identified as an important process for debris remobilization on the talus slopes. Veilleux et al. (2020) also highlighted the potential risks associated with the road that follows this slope.

Tasiapik Valley is located in the discontinuous permafrost zone and has a subarctic climate. Mean annual air temperature is −3 °C, −22.4 °C in February and 12.2 °C in July (data from Centre d'études nordiques (CEN) weather station at Umiujaq airport since 1999). Mean annual precipitation is approximately 500 mm, with 40% falling as snow (Ménard et al. 1998). The area is located at the edge of shrub and forest tundra zones; low shrubs, ericaceous plants and lichens cover the upstream part of the valley, whereas dense stands of

Fig. 1. Location of cameras in Tasiapik Valley and weather stations (A) (source of background image and hydrography: Ministère de l'Énergie et des Ressources naturelles (2019); source of transportation data: Ministère des Ressources naturelles et de la Faune (2019); Mapping tool: ArcGIS); oblique view toward the north, showing the cuesta frontslope on the southwest side (B); position of TAS1 camera near the cuesta ridgeline (C).

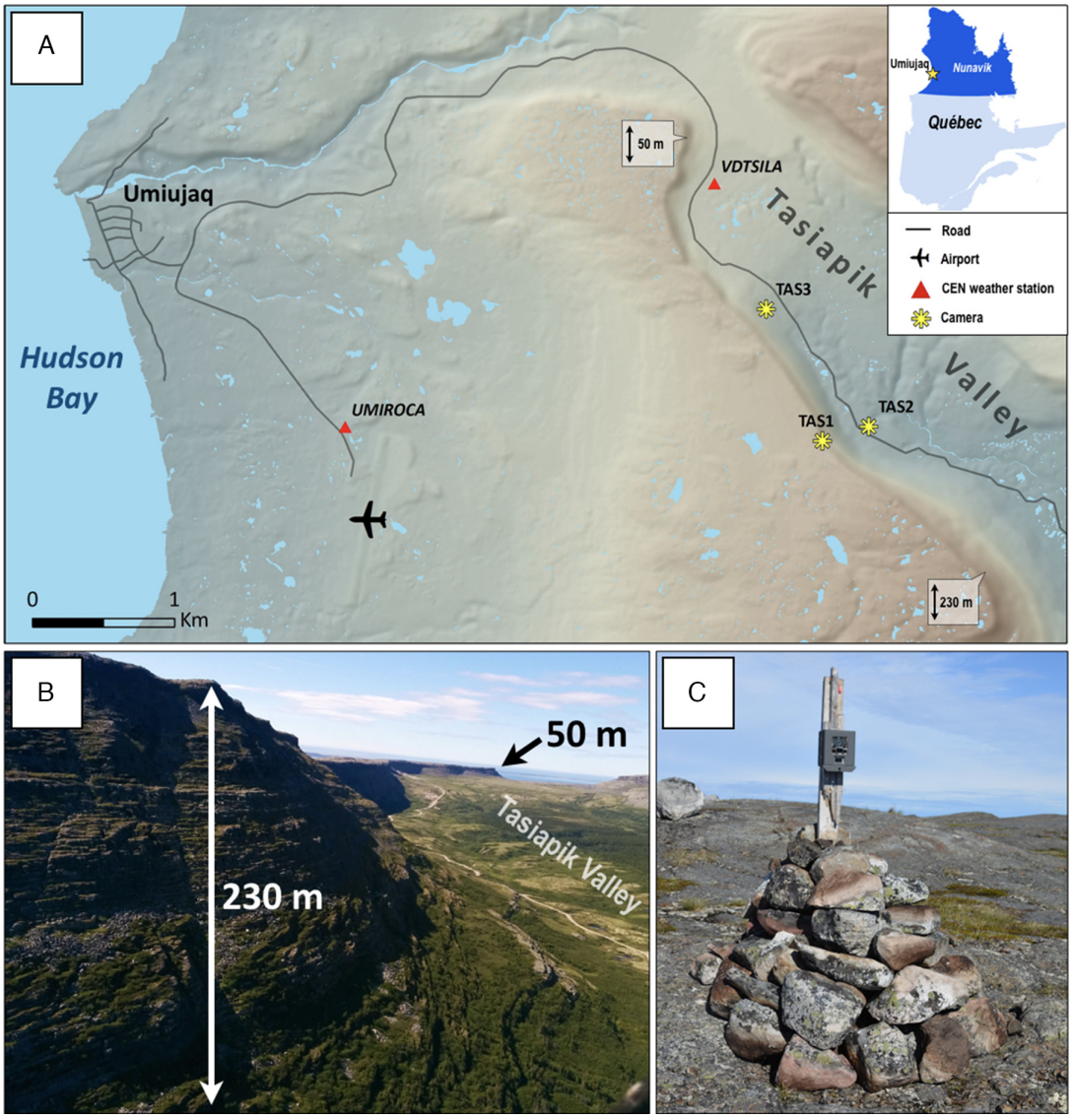

spruce cover the downstream part (Payette 1983; Allard and Seguin 1987; Provencher-Nolet et al. 2014; Pelletier et al. 2018).

Materials and methods

Time lapse cameras

Three Reconyx (Holmen, Wisconsin, USA) PC800 Hyperfire cameras were installed along the southwest side of Tasiapik Valley in August 2017. Camera TAS1 was installed at the top of the cuesta, providing a side view of the ridgeline, whereas cameras TAS2 and TAS3 were

positioned at the base of the talus slopes facing the rockwall, with fields of view measuring ~170 m high and ~95 m high, respectively. The cameras were inserted into a metal case attached with resistant staples to a pole that was inserted into the ground with rocks stacked at the base (Fig. 1C). The cameras took colour images with a 1080 p resolution (2048 × 1536). Images were taken every hour from 0900 to 1700 for the period between August 2017 and June 2018. The images covered a longer daytime period between June 2018 and August 2018, from 0600 to 2000, and were taken 15 or 30 min apart (depending on the camera location). In total, more than 14 000 photos were taken between 7 August 2017 and 15 August 2018. Each was analyzed individually to monitor the accretion/collapse of the snow cornice on images from camera TAS1 and to detect snow avalanche deposits on images from cameras TAS2 and TAS3. Observations of the snow cornice formation and evolution over the winter of 2017–2018 were only made at the camera TAS1 location, and do not apply for the entire crest length. The cameras provided data throughout the winter, but the spatial range was limited to the camera views.

Meteorological data

To contextualize the observations from the time lapse cameras, meteorological data from the SILA weather stations (CEN) were used. The VDTSILA station is located in the valley and UMIROCA station is located near the Umiujaq airport (CEN 2018). Detailed hourly air temperature, wind speed and direction, and precipitation (from the VDTSILA station only) data were examined, providing valuable information about the prevailing conditions occurring at specific moments or periods that were identified as being significant according to the results from the analysis of images. The 4–11 m/s interval suggested by Li and Pomeroy (1997) was used to contextualize snow transport with the wind speed.

Due to the malfunction of the VDTSILA station between late December and early February, precipitation data could not be recorded; data from the Kuujjuarapik station (160 km south of Umiujaq) were used instead. The authors acknowledge that meteorological data may not be entirely representative of the actual conditions on the investigated slope due to the location of the weather stations. In this regard, topography plays a major role, affecting temperature, wind, and precipitation distribution (i.e., elevation and shade); however, there was little evidence of snow avalanche events during this period.

Fieldwork

Photographs taken in situ during the summer and images taken by the time lapse cameras during the winter also helped to estimate snow depth, based on well-known scales (e.g., human scale, length and thickness of large boulders, height of vegetation, and height of the camera from the ground). Examination of snow avalanche deposits took place from 11 June to 16 June 2018. On-site characterization included measurement of the deposits and description of the shape of the track, the appearance (e.g., clean or dirty snow) and roughness (e.g., smooth or coarse snow surface). The dimensions of the deposits were determined using a handheld Garmin (Schaffhausen, Switzerland) Global Positioning System in the field and high-resolution satellite imagery and elevation data (from Québec's Ministère des Ressources Naturelles, de la Faune et des Parcs) in ArcGIS (ESRI, Redlands, California, USA). Moreover, we witnessed about 20 snow avalanches during fieldwork, allowing us to observe their flowing processes. Informal discussions with local residents helped us to better understand the occurrence of avalanches in the area and the prevailing meteorological conditions. This fieldwork complemented the data obtained from the cameras, by offering a visual corroboration of the snow avalanche dynamics at the scale of the valley, although only for a short period of time. Formal interviews will be conducted in a follow-up study.

Fig. 2. Meteorological conditions from 1 November to 20 November 2017, the cornice accretion period. Mean air temperature (A), snowfall (B), wind speed (C), and wind direction (D) are shown. Sources of meteorological data: CEN (2018), Environment Canada (2021).

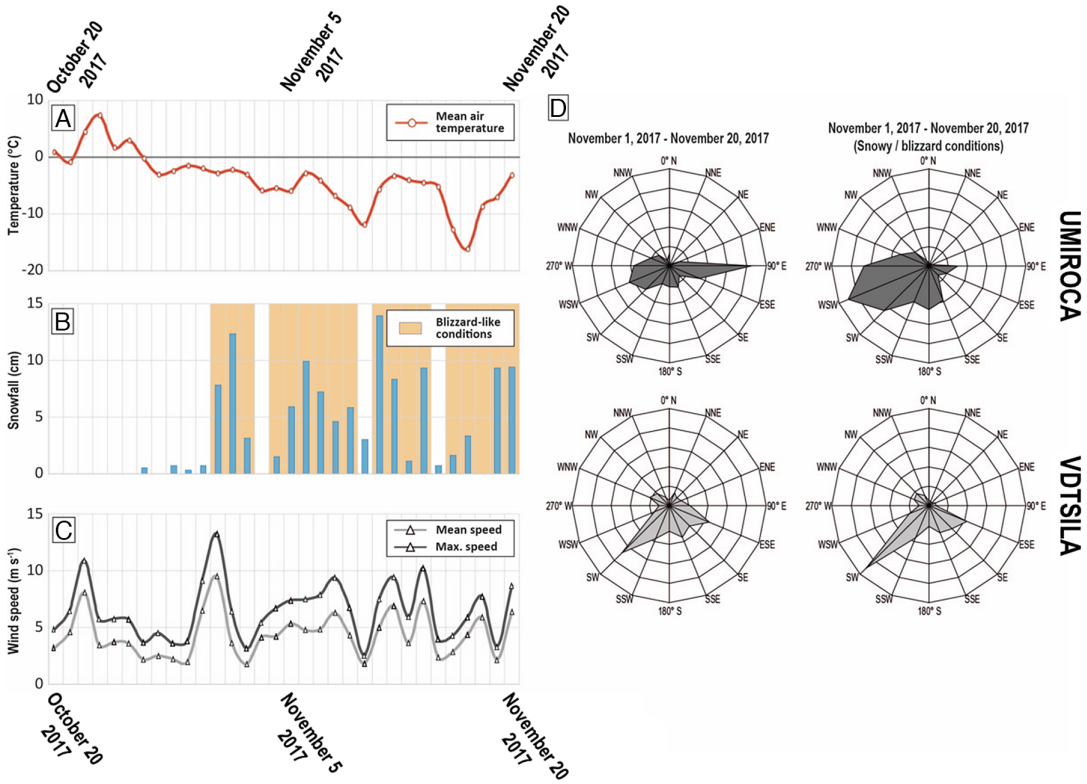

Results

Snow cornice development

Images from the camera TAS1, installed at the edge of the plateau, provided evidence of the formation of a snow cornice over the winter of 2017–2018. We were able to observe the initial accretion of the cornice from 1 November to 20 November, a period characterized by frequent blizzard conditions (Fig. 2), the first of the season. Snowfall totaled 118 cm during this period, whereas wind speed averaged 6.2 m/s, with maximum speed reaching up to 14 m/s. Data from the UMIROCA and VDTSILA stations indicated a predominantly south-westerly wind on snowy/blizzard days. The direction of these blizzard winds, almost perpendicular to the slope orientation (~212°) was, therefore, optimal for the formation and growth of a snow cornice. In addition, the wind enabled efficient snow transport toward the ridgeline due to the southwest orientation of the gently-inclined cuesta plateau and the virtual lack of obstacles to the wind.

After 20 November 2017, the cornice continued to expand gradually. Frequent drifting and blowing snow conditions occurred from November 2017 to May 2018 and evidence of snow displacement on the upwind cuesta plateau was observed, such as sastrugi formation. Oriented with the southwesterly prevailing winds, the irregular dune-shaped features formed parallel ripples facing northeast. Wind data from the UMIROCA station showed that from 1 November 2017 to 1 June 2018, 67.9% of total days had an average wind speed between 4 and 11 m/s, and 81.6% of total days had a maximum wind speed within this interval. This

Fig. 3. Schematic cross-sections and photographs of the snow cornice during the accretion, creeping and collapsing/melting periods. Measurements shown are estimated, based on well-known scales in the field (e.g., human scale, length and thickness of large boulders, height of vegetation, and height of the camera from the ground).

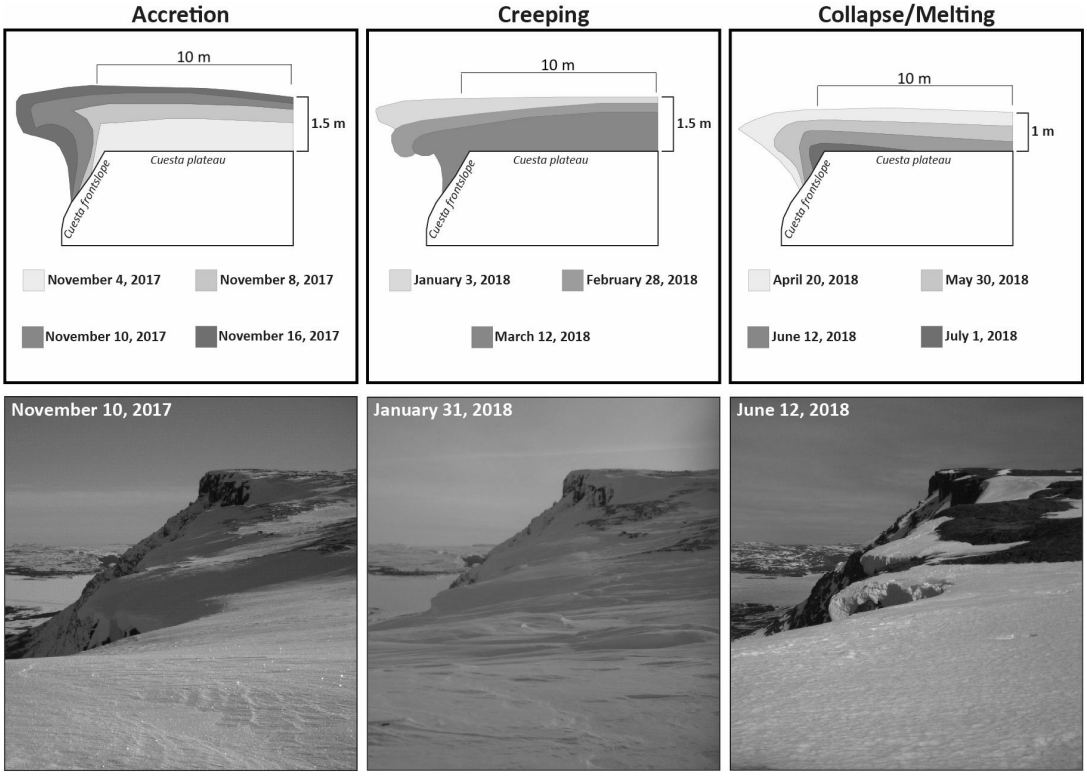

denotes the efficient wind speed for dry snow transport in Arctic regions, which is favourable for the formation and growth of snow cornices (Li and Pomeroy 1997; McClung and Schaerer 2006). Wind direction was efficient for 48.3% of the days in the same period, considering the west–northwest to south–southeast direction range for efficient snow supply to the cornice. Northeast–southwest-oriented sastrugi on the snow surface highlight the continuous snow transport and erosion by wind throughout winter until the end of May 2018.

Snowpack thickness, estimated from the photographs, was variable on the cuesta plateau, as depressions collected up to 1.5 m of snow, whereas windswept higher ground remained bare rock. Continuous wind-driven snow supply toward the cornice compensated for low snow precipitation from January to March 2018, which totaled only 50.7 cm. During this period, south–southeast to south–southwest prevailing winds contributed to the widening of the cornice, later resulting in its progressive deformation. The overhanging portion started tilting and creeping (Fig. 3), which was also observed on the camera TAS2 from the base of the slope. No cornice failure was observed before March as the snow cover in the upper part of the slope directly below the cornice remained intact. Thereafter, failures occurred more frequently, especially from late May through June.

Snow avalanche events documented from the time lapse cameras

Most of the snow avalanches caught on camera (36 of a total of 39 events) were observed on the camera TAS2, located in front of a wide talus slope at the base of a 200 m high

Fig. 4. Snow avalanche events identified on TAS2 camera from November 2017 to June 2018, subdivided into six periods for clarity. Dotted lines represent estimated snow avalanche extent due to poor visibility. Black line shows the position of the road in each image.

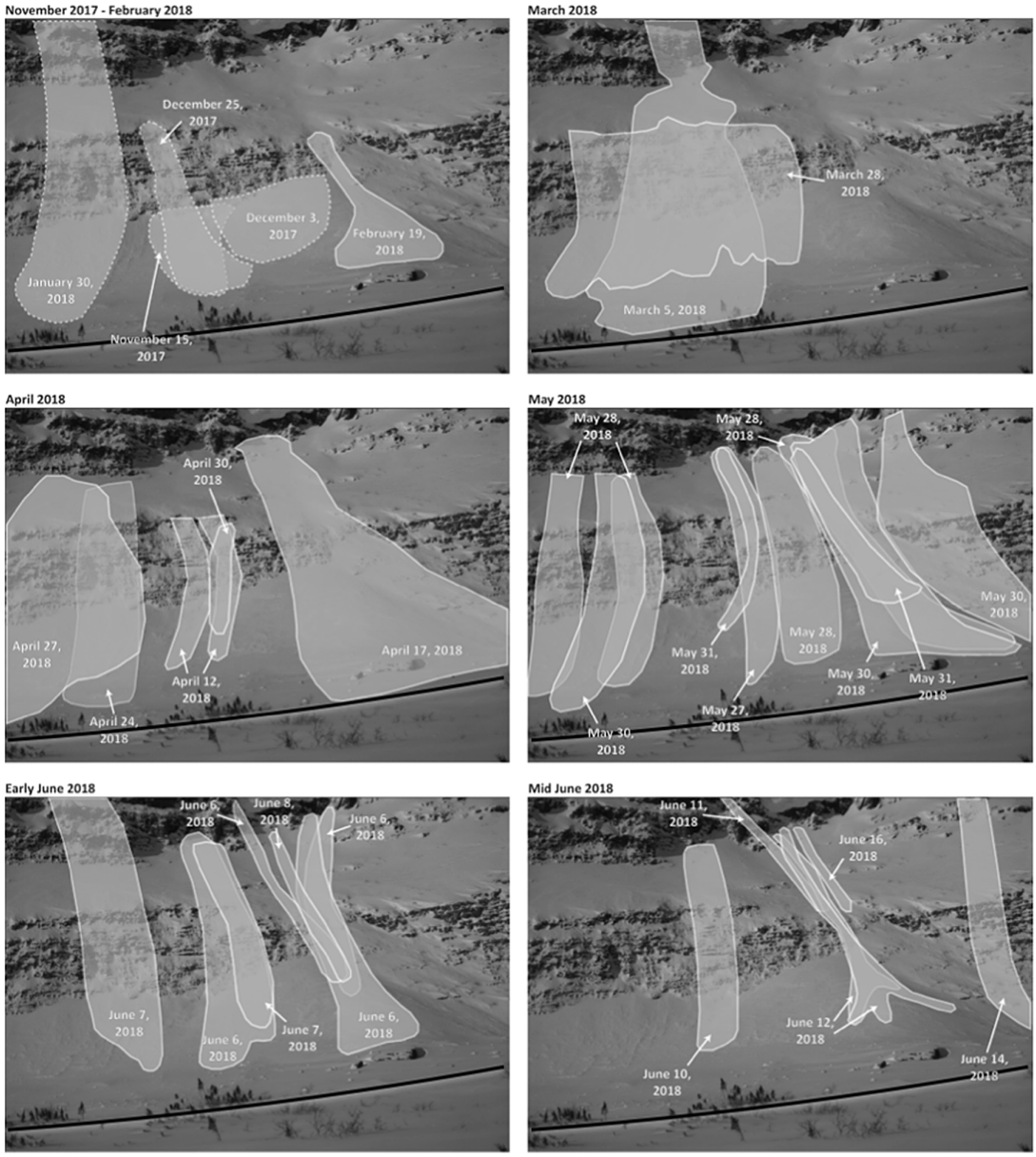

rockwall in the downstream part of the valley (Supplementary Table S1[1]). Multiple avalanches occurred at the same location only a couple of days apart, as shown by the overlapping avalanche tracks on Fig. 4; however, the tracks were rapidly hidden by fresh snow and wind erosion. When combined together, the repeated snow avalanches over this slope

[1]Supplementary material is available with the article at https://doi.org/10.1139/as-2020-0013.

enabled the identification of snow avalanche paths of various sizes. Only three events were observed on the camera TAS3 located upstream: on 26 April, 28 April, and 28 May 2018, respectively.

On the camera TAS2, five events were identified before March 2018, occurring respectively on 15 November 2017, 3 December 2017, 25 December 2017, 30 January 2018, and 19 February 2018 (Fig. 4). Low visibility made it difficult to clearly distinguish the types and dimensions of snow avalanches that occurred during this period. However, snowballs rolling on the snow-covered talus slope or small loose-snow avalanches were observed in November and December 2017, but these were not likely triggered by solar radiation at that time of the year. A slab avalanche occurred between 1700 on 4 March 2018 and 0900 on 5 March 2018, leaving a clear crown and bed surface in the uppermost part of the slope. This event was triggered by a cornice collapsing on the same day and in the same time interval, as confirmed by the camera TAS1. Loose snow avalanches, initiated at mid-slope, occurred in late March 2018 and early April 2018. On 17 April 2018 between 1100 and 1200, a snow avalanche occurred after the failure of a large portion of the cornice. A distinct scarp left by the collapsing cornice was visible, as well as the space left vacant by the tilted roll face of the cornice. In addition, angular snow blocks were visible within the deposit that reached the road, which indicates that dry snow was involved. Another snow avalanche that initiated at the top of the slope occurred on 24 April 2018; however, there was no visible evidence of a fallen cornice and the deposit consisted of dry snow blocks partly rounded by the longer runout. From 27 May 2018 to 16 June 2018, a total of 25 snow avalanche events occurred. Every cornice failure during this period was synchronized with wet snow avalanche deposits, as observed on the cameras.

According to the UMIROCA and VDTSILA climate stations, winter — dry snow — conditions prevailed prior to 27 May 2018; maximal and minimal daily air temperatures remained below 0 °C and the majority of precipitation fell as snow. Only one rain episode (1.0 mm) occurred on 5 December 2017 (Fig. 5). Beginning on 27 May 2018, warmer temperatures and abundant rainfall episodes combined to cause multiple cornice failures and wet snow avalanches over the following days. A total of eight snow cornice failures and 23 snow avalanche events were observed until 16 June. Thereafter, no snow avalanche events were observed, although sporadic falls of rock debris occurred as well as debris sliding on the snow-covered talus. Rapid melting of the snow led to the retreat of the cornice and no failures occurred during this period. Ephemeral meltwater streams were observed in late June and July on the slope, flowing down from the ridgeline to the talus slopes.

Snow avalanches were frequent during fieldwork from 11 to 16 June 2018. At least 20 events were witnessed in real-time, the majority of which were triggered by cornice failures, which generated a very audible sound throughout the valley. Heavy rainfall (13.1 mm) on 11 June followed by five days of good weather with no measurable precipitation and temperature above 0 °C increased the downward motion of the cornice and, thus, enabled the cornice failures. The meteorological conditions on 11 June were similar to those prevailing on 27 May and the following days, when numerous snow cornice failures and snow avalanches were observed on the cameras TAS1 and TAS2.

Wet and dry snow avalanche deposits in spring 2018

A total of 29 deposits were identified during fieldwork in June 2018, extending along the entire length of the southwest side of the valley (Fig. 6, Supplementary Fig. S1[1], and Supplementary Table S2[1]), whereas no deposit was observed on the opposite northeast side as the snow cover had melted considerably by that time. Runout zones were clearly outlined for all snow avalanche deposits; the starting zone and track were sometimes hard to identify over bare rockface sections as the snow had completely melted on the steepest

Fig. 5. Occurrence of cornice failures and snow avalanches during the winter/spring of 2017–2018, as observed on TAS1 and TAS2 cameras. Maximum air temperature and precipitation are also shown (source: CEN 2018, Environment Canada 2021).

Fig. 6. Oblique 3D view of the southwest side of Tasiapik Valley, highlighting the snow avalanche deposits observed in the field in June 2018 (A) (source of background image: CEN 2010; Mapping tool: ArcGIS). Topographic long profiles for snow avalanche deposits respectively located down-valley (B), mid-valley (C), and up-valley (D).

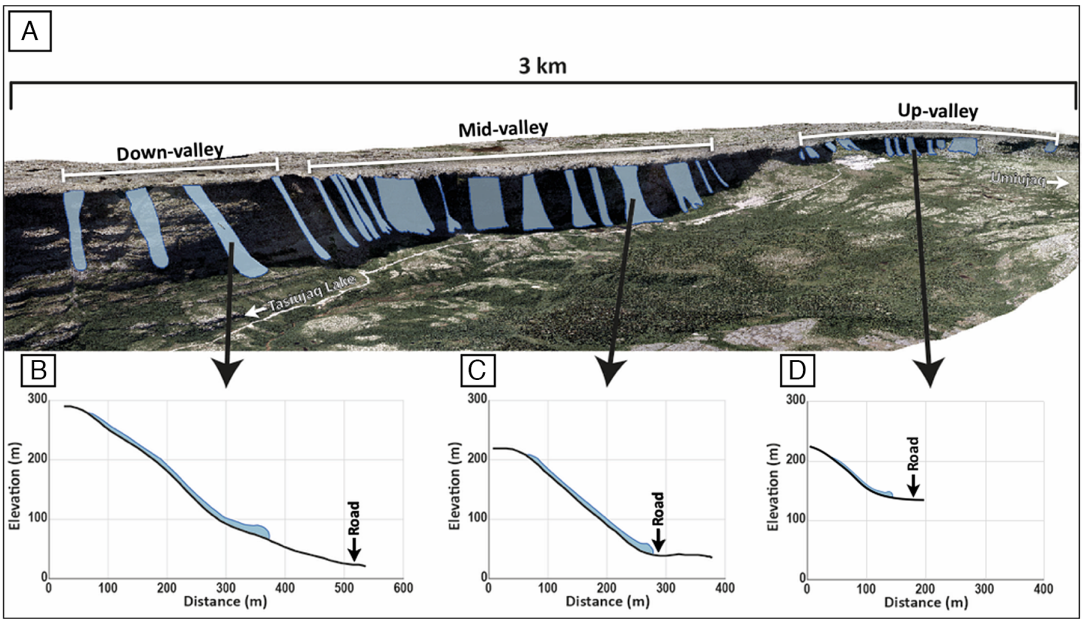

parts of the slope. A snow cornice was still visible along most of the cuesta ridgeline, although it had considerably receded in the previous weeks, according to the images from the camera TAS1.

Not all of the snow avalanches reached the road in the runout zone located mid-valley (Fig. 7). However, the deposits found there consisted of wet snow packed against the road embankment with incorporated rocky debris, giving a dirty appearance to the deposits. The deposits generally exhibited a lobate shape, but some also had a multilobate shape (Fig. 7). By comparison, deposits observed on the photos taken by the cameras TAS2 and TAS3 before 27 May did not appear to have incorporated debris, originating either from loose snow, slab avalanches, or snow cornice failures, and flowing mostly over the snow surface.

Snow avalanche deposits located down-valley showed an elongated form (width/length ratio of 0.15), extending from the snow cornice down to a rocky outcrop located mid-slope. Runout distances ranged between 275 and 350 m, and the mean runout angle (alpha angle) was 37.2°. The width of the snow deposits ranged from 28 to 80 m ($\overline{x} = 47$ m).

The steeper slope mid-valley led to less snow accumulation, and snow avalanche tracks were not always visible. However, the snow cover was still sufficient in the uppermost part of the slope to identify the starting zone. Various deposit forms were observed, including elongated, fan-shaped, juxtaposed, and coalescent deposits, as shown in Figs. 4 and 6A. Runout distances ranged from 120 to 260 m, with a mean runout angle of 44.2°. The width ranged from 12 to 140 m ($\overline{x} = 47$ m) and mean width/length ratio was 0.26.

In the upstream part of the valley, a lower height and gentler slope helped to preserve the snow cover, but also led to shorter runout distances, ranging from 49 to 112 m, with a mean runout angle of 31.2°. The width ranged from 16 to 140 m ($\overline{x} = 40$ m), with a mean

Fig. 7. Comparison between the shorter runout distance from a wet snow avalanche on 12 June 2018 (A), a larger wet snow avalanche with a longer runout in late May 2018 (B), and a large slab avalanche in April 2018 (C). Photo taken by TAS2 camera on 12 June 2018.

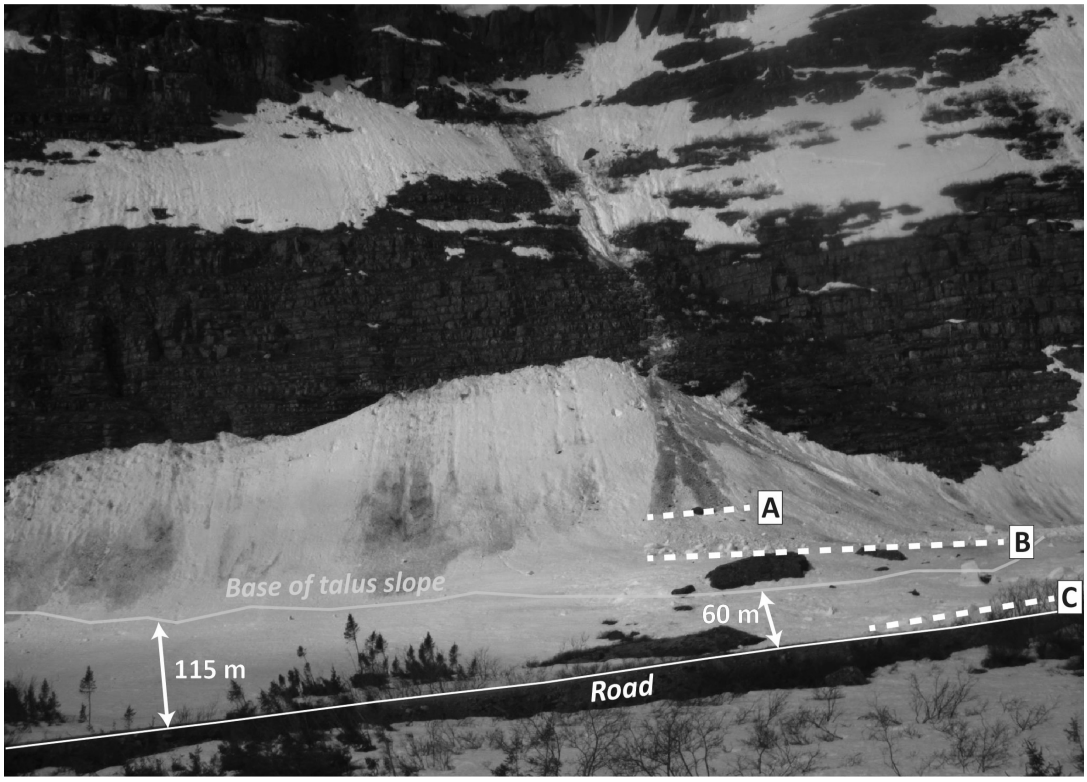

width/length ratio of 0.52. Deposits exhibited a short lobate shape, with large (up to 5 m long) snow blocks with sharp edges found in the runout zone. These blocks provide evidence of cornice failures in this portion of the valley, as the shape of the snow blocks indicates the presence of solid ice at that time of the year. In addition, several snow cover destabilizations on the uppermost part of the slope (drifted snow accumulations on the lee side of the upper rock face) released many micro snow avalanches in the form of small scale snowballs (<100 cm diameter in the deposition zone), indicating wet snow that rolled down the snow-covered slope, leaving well-defined tracks.

As noted above, the proximity of the road to the slope demonstrates the potential risk associated with snow avalanches and other slope processes. For instance, many fallen angular cobbles and boulders (up to 50 cm in long axis), later transported by snow avalanches, could be found near the road embankment. The observation of several boulders at this location shows that snow avalanches have already had a significant impact in the area. The average distance measured between the snow avalanche deposits and the road was 112.2 m, with generally greater distances down-valley (235 m) and shorter distances up-valley (85 m). However, the snow avalanche event of 17 April 2018 did reach the road (as observed on the camera TAS2), and another mid-valley event on 12 June 2018 extended to within a few metres from the road (Fig. 8). Although the road is not plowed during the winter, it is still used by snowmobiles and ATVs. Many vehicles were observed travelling on the road all winter long in the photos taken by the camera TAS2.

Fig. 8. Wet avalanche deposits with runout distances near the road. Photo taken on 12 June 2018.

Discussion

Meteorological and topographic control

The results have demonstrated that meteorological conditions enabled continuous snow transport toward the cuesta ridgeline, favouring the development of a snow cornice in November 2017 over a period of 248 days. From December onwards, efficient wind speed and direction compensated for the low amount of snow precipitation due to the freezing of Hudson Bay, which induced a more continental climate (Wilson 1971), as previously reported in subarctic environments by Germain (2016).

McCarty et al. (1986) suggested that snow cornices are sensitive to rapidly changing conditions, especially during spring, as they become isothermal (no temperature gradient within the snow cover, generally at 0 °C), weakening the bonds between snow particles. Snow cornices can also be subjected to large temperature variations between day and night (Burrows and McClung 2006) and rain episodes (Vogel et al. 2012) that favour failures. Accordingly, in late May 2018, the maximum daily air temperature had risen above 0 °C and precipitation shifted from snow to rain, likely causing the multiple failures recorded during this period. For instance, on 27 May 2018, the air temperature reached 5.4 °C, whereas rainfall totaled 21 mm; five failures of the snow cornice were recorded in the subsequent four days. This rain event, combined with warmer temperatures, contributed to the overloading of the cornice, which tilted significantly during those days. The effect of longer daylight in spring could also have exacerbated the meteorological control of warm temperature and rain on the cornice. Prior to March, the snow cover in the uppermost part of the slope directly below the cornice remained intact, suggesting that no failure occurred or that failures were infrequent and concerned only a limited amount of snow. A similar temporal pattern was observed by Vogel et al. (2012) and Eckerstorfer et al. (2013) in Spitsbergen, with a strong propensity for cornice failures in the spring.

As is the case in many mountain snowpacks, blowing snow accumulation on the lee side slope favoured the formation of a wind slab (McClung and Schaerer 2006). The northeast-oriented slope also benefits from extensive shade, especially in winter when daylight is minimal. A similar slope orientation and wind condition were reported by Lied and Domaas (2000) on the southwest slope in Kangiqsualujjuaq (Nunavik), where the 1999 deadly snow avalanche occurred. These factors induce the development and preservation of weak snow layers that are prone to snow avalanches (McClung and Schaerer 2006). During the spring of 2018, a synchronicity between cornice failures and snow avalanches was observed, as the first most likely triggered the second. Similarly, most snow avalanches observed during fieldwork in June 2018 were triggered by collapsing cornices.

Snow avalanche runout and proximity to the road

As mentioned earlier, the road passing through Tasiapik Valley is used by local residents travelling with snowmobiles and ATVs. The fact that snow avalanches reached the road at least twice during the winter of 2017–2018 means that we must regard these two snow avalanche paths as dangerous for residents during the winter. Ongoing snow avalanche investigation in Tasiapik Valley could provide evidence of several other hazardous snow avalanche paths in the near future.

Wet snow avalanches had limited runout, especially mid-valley, due to their relatively slow movement and the abrupt transition between the slope and the valley floor. The change in slope angle from ~74° to ~4° causes the rapid deceleration of the wet snow avalanche and compaction of the snow in the runout zone (McClung and Schaerer 2006), which explains the high alpha angles. Farther down-valley near Tasiujaq Lake, deposits were located far from the road and the terrain separating them is virtually flat; the runout is also notably shorter than other deposits from snow avalanches that occurred earlier in the spring. The multilobate shape was attributable to the high water and debris content of the deposit, similar to a mudslide (Jomelli and Bertran 2001). Due to their flow in direct contact with the ground, their erosive capacity on the rockwall is stronger (Gardner 1983; McClung and Schaerer 2006) and most of the wet snow avalanche deposits contained dirty and dense snow, incorporating mainly fine particles (i.e., gravel and pebbles), but also boulders, which could potentially endanger people travelling on the road or nearby. Moreover, the presence of talus slopes at the foot of the rockwall indicates the occurrence of rockfalls in the area (Veilleux et al. 2020). Minor sporadic rockfalls occurred in early June 2018 during the peak period of snow avalanche activity, showing the potential and episodic synchronicity of both slope processes. It is also likely that snow avalanches played an important role in supplying debris for the numerous talus slopes in Tasiapik Valley.

Limitations of the study

The use of time lapse images to monitor slope processes and evolution has been adopted in other mountainous/cold regions such as Spitsbergen (e.g., Vogel et al. 2010), the Swiss Alps (e.g., van Herwijnen et al. 2013), Norway (e.g., Laute and Beylich 2014), and the western United States (e.g., Munroe 2018). Although the images provide valuable information about snow conditions and snow avalanches, the use of cameras in Arctic regions presents some challenges in winter due to low daylight and harsh weather conditions, resulting in numerous unusable images (i.e., frost, blowing snow, low sunlight/shade) during daylight. In this study, conditions of poor visibility often occurred on multiple consecutive days, which means that snow avalanche events could have been missed due to drifting snow rapidly covering the snow deposit surface, wind erosion of the snow surface and sublimation. In addition, the cameras TAS2 and TAS3 only have a ~200 m wide range of vision, representing a limited sample of the valley's 5 km long southwest side. The conditions could have been

locally favourable (i.e., numerous events observed on camera TAS2) or unfavourable (i.e., very few events observed on camera TAS3) for cornice failures and snow avalanches, although it is impossible to extrapolate these events (or non-events) at the valley scale. Data collected and analyzed at this time also only covers one winter and, thus, it is impossible to obtain an interannual pattern at this stage. The final consideration concerns the meteorological data from the UMIROCA and VDTSILA stations. As the first is located at Umiujaq airport and the second is located on the valley floor, both stations do not reflect the actual conditions occurring near the ridgeline. Due to higher elevation and the ridge-like position, temperatures could be colder than nearby Umiujaq or the valley floor, and the wind could be stronger, as experienced in the field.

Conclusion

This study has outlined the occurrence of snow avalanche events during the winter of 2017–2018 in Tasiapik Valley with the use of automatic time lapse cameras. Despite the limitations mentioned above, the results have provided evidence of favourable meteorological and topographic conditions for the development of a snow cornice at the top of the southwest side of the valley and the triggering of multiple snow avalanches. A strong propensity for spring (May–June) wet snow avalanches was observed, resulting from a rapid shift in weather conditions. During the same period, frequent cornice failures triggered snow avalanches. These observations were confirmed by in-situ investigation of snow avalanche deposits in June 2018. Photo-monitoring has helped us to better understand the slope dynamics over a one-year span. Further camera monitoring for the years to come is required to assess the interannual recurrence of snow cornice formation/failure and snow avalanche triggering. From informal discussions with local residents in Umiujaq, we were told that the 2017–2018 winter was particularly long and harsh, which could have triggered more snow avalanches than usual. Formal interviews will be conducted in a follow-up study to further assess the potential risk associated with snow avalanches in the area.

Acknowledgements

Funding for this project was provided by the Natural Sciences and Engineering Research Council of Canada (NSERC), IPEV DeSiGN, LabEx DRIIHM (French program “Investissements d’Avenir” — ANR-11-LABX-0010 — managed by the French National Research Agency, ANR) and OHMi NUNAVIK-TUKISIG. Thanks are extended to the community of Umiujaq for its ongoing support. The authors also want to thank Félix Faucher, Julien Lebrun, and Þorsteinn Saemundsson for their valuable help in the field, and the Centre d’études nordiques (CEN) for logistical support.

References

Allard, M., and Seguin, M.K. 1987. The Holocene evolution of permafrost near the tree line, on the eastern coast of Hudson Bay (northern Quebec). Can. J. Earth Sci. **24**(11): 2206–2222. doi: 10.1139/e87-209.

ARK. 2007. Projet de parc national des Lacs-Guillaume-Delisle-et-à-l’Eau-Claire. État des connaissances. Administration régionale Kativik, Service des ressources renouvelables, de l’environnement, de territoire et des parcs, Section des parcs, Kuujjuaq, Québec, Canada.

Burrows, R., and McClung, D.M. 2006. Snow cornice development and failure monitoring. *In* International Snow Science Workshop, Telluride, Colo., USA. Vol. 101, 21920.

CEN. 2010. UMI_orthomosaic 15 cm. Centre d’études nordiques, Université Laval, Québec, Québec, Canada.

CEN. 2018. Climate station data from the Umiujaq region in Nunavik, Quebec, Canada, v. 1.6 (1997–2018). Nordicana D9. doi: 10.5885/45120SL-067305A53E914AF0.

Chandler, F.W. 1988. The early Proterozoic Richmond Gulf Graben, East Coast of Hudson Bay, Quebec. Vol. 362. Geological Survey of Canada.

Chandler, F.W., and Schwarz, E.J. 1980. Tectonics of the Richmond Gulf area, northern Quebec — a hypothesis. Current Research, Part C. Geological Survey of Canada. Paper No. 80. pp. 59–68. doi: 10.4095/102176.

Dionne, J.C. 1976. Les grandes cuestas de la mer d’Hudson. GÉOS, **5**(1): 18–20.

Eaton, D.W., and Darbyshire, F. 2010. Lithospheric architecture and tectonic evolution of the Hudson Bay region. Tectonophysics, **480**(1–4): 1–22. doi: 10.11575/PRISM/35077.
Eckerstorfer, M., Christiansen, H.H., Rubensdotter, L., and Vogel, S. 2013. The geomorphological effect of cornice fall avalanches in the Longyeardalen valley, Svalbard. Cryosphere, **7**(5): 1361–1374. doi: 10.5194/tc-7-1361-2013.
Environment Canada. 2021. Historical data — Umiujaq. Available from https://climate.weather.gc.ca/historical_data/search_historic_data_e.html.
Gardner, J.S. 1983. Observations on erosion by wet snow avalanches, Mount Rae area, Alberta, Canada. Arct. Alp. Res. **15**(2): 271–274. doi: 10.2307/1550929.
Germain, D. 2016. Snow avalanche hazard assessment and risk management in northern Quebec, eastern Canada. Nat. Hazards, **80**(2): 1303–1321. doi: 10.1007/s11069-015-2024-z.
Guimont, P., and Laverdière, C. 1980. Le sud-est de la mer d'Hudson : un relief de cuesta. *In* The coastline of Canada. *Edited by* S.B. McCann. Geological Survey of Canada. Paper 80-10. pp. 303–309.
Hétu, B. 2001. Une géomorphologie socialement utile : la question des risques naturels. *In* Géographie et société : vers une géographie citoyenne. *Edited by* S. Laurin and J.-L. Klein. Presses de l'Université du Québec, Québec, Québec, Canada. pp. 61–92. doi: 10.2307/j.ctv18pgq9z.
Jomelli, V., and Bertran, P. 2001. Wet snow avalanche deposits in the French Alps: structure and sedimentology. Geogr. Ann.: Ser. A, Phys. Geogr. **83**(1–2): 15–28. doi: 10.1111/j.0435-3676.2001.00141.x.
Laute, K., and Beylich, A.A. 2014. Morphometric and meteorological controls on recent snow avalanche distribution and activity at hillslopes in steep mountain valleys in western Norway. Geomorphology, **218**: 16–34. doi: 10.1016/j.geomorph.2013.06.006.
Li, L., and Pomeroy, J.W. 1997. Estimates of threshold wind speeds for snow transport using meteorological data. J. Appl. Meteorol. **36**(3): 205–213. doi: 10.1175/1520-0450(1997)036<0205:EOTWSF>2.0.CO;2.
Lied, K., and Domaas, U. 2000. Avalanche hazard assessment in Nunavik and on Côte-Nord, Québec, Canada. Norwegian Geotechnical Institute.
McCarty, D., Brown, R.L., and Montagne, J. 1986. Cornices: their growth, properties, and control. *In* 1986 International Snow Science Workshop, Lake Tahoe, Calif., USA. pp. 41–45.
McClung, D., and Schaerer, P.A. 2006. The avalanche handbook. The Mountaineers Books.
Ménard, É., Allard, M., and Michaud, Y. 1998. Monitoring of ground surface temperatures in various biophysical micro-environments near Umiujaq, eastern Hudson Bay, Canada. *In* Proceedings of the 7th International Conference on Permafrost, Yellowknife, N.W.T., Canada. pp. 723–729.
Ministère de l'Énergie et des Ressources naturelles. 2019. Cartes topographiques des villages autochtones du nord à l'échelle de 1/2 000. Direction générale de l'information géospatiale, Québec, Québec, Canada. Available from https://www.donneesquebec.ca/recherche/dataset/cartes-topographiques-des-villages-autochtones-du-nord-a-l-echelle-de-1-2-000.
Ministère des Ressources naturelles et de la Faune. 2019. Cartes topographiques des villages autochtones du nord à l'échelle de 1/2 000. Direction générale de l'information géospatiale, Québec, Québec, Canada. Available from https://www.donneesquebec.ca/recherche/dataset/cartes-topographiques-des-villages-autochtones-du-nord-a-l-echelle-de-1-2-000.
Munroe, J.S. 2018. Monitoring snowbank processes and cornice fall avalanches with time-lapse photography. Cold Reg. Sci. Technol. **154**: 32–41. doi: 10.1016/j.coldregions.2018.06.006.
Payette, S. 1983. The forest tundra and present tree-lines of the northern Québec-Labrador peninsula. Nordicana, **47**: 3–23.
Pelletier, M., Allard, M., and Levesque, E. 2018. Ecosystem changes across a gradient of permafrost degradation in subarctic Québec (Tasiapik Valley, Nunavik, Canada). Arct. Sci. **5**(1): 1–26. doi: 10.1139/as-2016-0049.
Provencher-Nolet, L., Bernier, M., and Lévesque, E. 2014. Quantification des changements récents à l'écotone forêt-toundra à partir de l'analyse numérique de photographies aériennes. Écoscience, **21**(3–4): 419–433. doi: 10.2980/21-(3-4)-3715.
Stockwell, C.H., McGlynn, J.C., Emslie, R.F., Sanford, B.V., Norris, A.W., Donaldson, J.A., et al. 1979. Géologie du Bouclier canadien. *In* Géologie et ressources minérales du Canada. *Edited by* R.J.W. Douglas and L.P. Tremblay. Energie, mines et ressources Canada. pp. 117–119.
van Herwijnen, A., Berthod, N., Simenhois, R., and Mitterer, C. 2013. Using time-lapse photography in avalanche research. *In* Proceedings of the International Snow Science Workshop. pp. 950–954.
Veilleux, S., Bhiry, N., and Decaulne, A. 2020. Talus slope characterization in Tasiapik Valley (subarctic Québec): evidence of past and present slope processes. Geomorphology, **349**: 106911. doi: 10.1016/j.geomorph.2019.106911.
Vogel, S., Eckerstorfer, M., and Christiansen, H.H. 2010. Cornice dynamics above Nybyen in Svalbards high arctic landscape. *In* Proceedings of the International Snow Science Workshop. pp. 785–790.
Vogel, S., Eckerstorfer, M., and Christiansen, H.H. 2012. Cornice dynamics and meteorological control at Gruvefjellet, Central Svalbard. Cryosphere, **6**(1): 157–171. doi: 10.5194/tc-6-157-2012.
Wilson, C. 1971. Atlas climatologique du Québec. Service de l'Environnement Atmosphérique du Canada, Toronto, Ontario, Canada.